ARMY RESEARCH LABORATORY

CREATION Scene Generation for ATR Applications

by Hung M. Nguyen, Joseph A. Penn, Teresa A. Kipp,
Giap D. Huynh, and Janice F. Colby

ARL-TR-1489 April 1998

Approved for public release; distribution unlimited.

The findings in this report are not to be construed as an official Department of the Army position unless so designated by other authorized documents.

Citation of manufacturer's or trade names does not constitute an official endorsement or approval of the use thereof.

Destroy this report when it is no longer needed. Do not return it to the originator.

Army Research Laboratory
Adelphi, MD 20783-1197

ARL-TR-1489 **April 1998**

CREATION Scene Generation for ATR Applications

Hung M. Nguyen, Joseph A. Penn, Teresa A. Kipp, Giap D. Huynh, and Janice F. Colby
Sensors and Electron Devices Directorate

Approved for public release; distribution unlimited.

Abstract

The CREATION (computer generation of realistic environments with atmospheres for thermal imagery with optics and noise) scene simulation program produces high-quality three-dimensional imagery of realistic battlefield environments.

Several important methodologies used in the CREATION program are discussed. These include efficient ground-texturing techniques that use growth-rule-based texture patterns and gradient-of-steepest-descent algorithmic erosion processes to increase the realism of low-resolution Defense Mapping Agency (DMA) digital terrain elevation data (DTED). Methods discussed include algorithms to produce very realistic three-dimensional trees that are succinctly described by a small number of geometrical parameters and efficiently rendered. Discussion of the vegetation model also includes a description of algorithms to efficiently render large masses of trees that smoothly and seamlessly increase in detail as the viewer continuously approaches them.

Contents

Figures

Tables

1. Introduction

The objective of the CREATION scene generation software is to simulate realistic, multispectral, three-dimensional scenes (e.g., infrared (IR), visible, etc) of diverse geographical locations and environmental conditions. The intent is to reduce the Army's dependence on field-collected data by using validated and verified synthetic scene generation methodologies to supplement real data for many applications. These applications include the development, testing, and evaluation of automatic target recognizer (ATR) algorithms; image clutter metrics research; signature phenomena research; mission planning; training; human perception study; and multispectral sensor modeling.

2. General Design of Creation

The CREATION simulation model consists of several programs developed in-house that integrate and interface with various existing target geometry, terrain surface data, and thermal prediction models. These programs combine to form an extremely powerful research tool. The internally developed software includes the feature editor (FED) and the CREATION scene generator program, which includes the graphics user interface, vegetation model, surface-texturing processes, and atmospheric and sensor simulation models. The relationship of CREATION to other models and to its constituent parts is shown in figure 1.

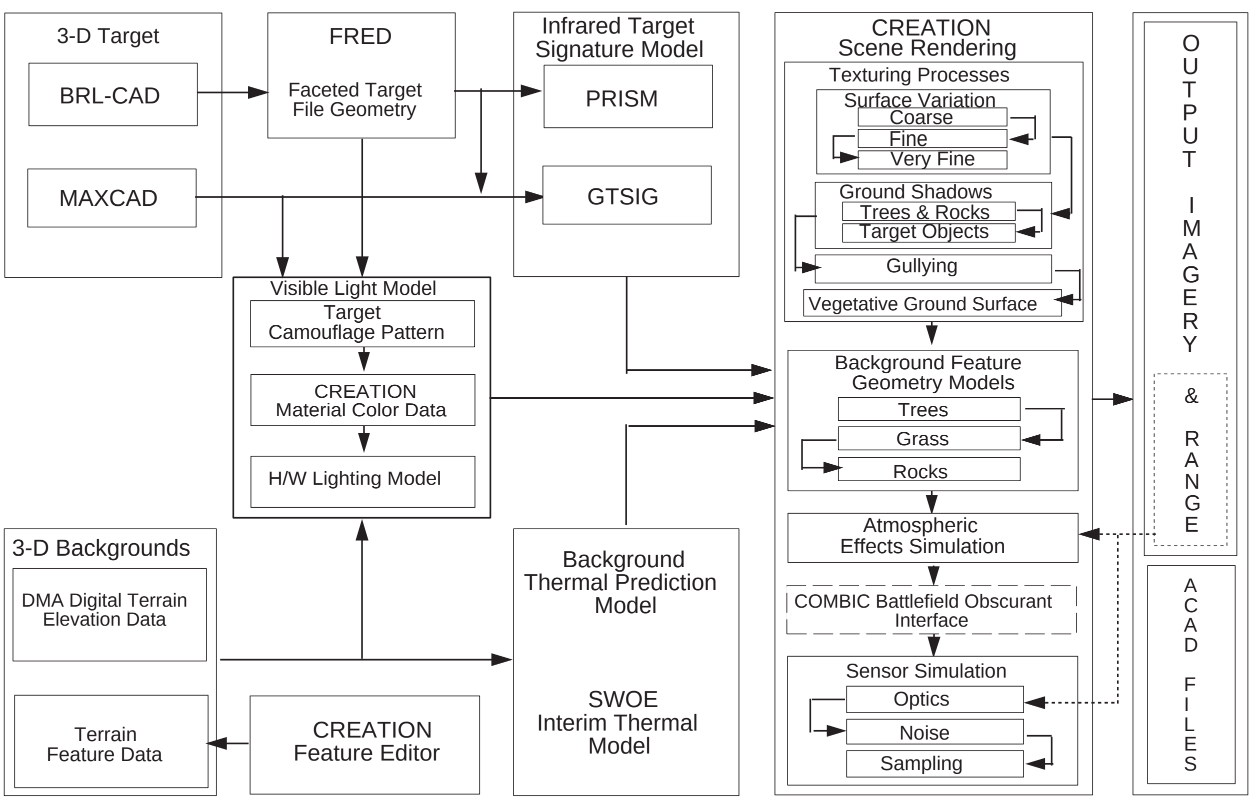

Figure 1. Overview of CREATION scene generation process.

2.1 External Models and Input Databases

The CREATION scene generator requires existing, externally generated data files to create simulations of specific geographical locations and scenarios. The following data are produced by other programs and processes:

- Digital terrain elevation data (DTED) [1] are the standard, digitally formatted Defense Mapping Agency (DMA) surveyed data, which consist of an array of elevations sampled at either 30- or 100-m intervals. These data are used to generate the topographic basis on which the vegetation, soils, roads, etc, are applied.
- Target geometry files are obtained from either (a) Ballistic Research Laboratory computer-assisted design (BRL-CAD) [2] combinatorial solid geometry (CSG) files that are converted to faceted geometry via the Faceted Region Editor (FRED) [3] from the Tank Automotive Research, Development, and Engineering Center (TARDEC) or (b) the MAXCAD faceted geometry files from Georgia Technological Research Institute (GTRI).
- Target thermal-prediction files are generated with either (a) the physically reasonable infrared signature model (PRISM) [4] via target geometries converted by FRED or (b) GTSIG (Georgia Tech IR signature code) [5] with MAXCAD target geometry input data files. The thermal-prediction files must be generated in association with the desired scenario, i.e., the physical location, target operating state (velocity, orientation, running time, etc), and meteorological conditions, to realistically simulate the temperature profile.
- Background thermal-prediction files are created using the interim thermal model (ITM) from the Smart Weapons Operability Enhancement (SWOE) program and the Waterways Experiment Station (WES) [6,7]. This model uses meteorological data to predict the temperature profiles of vegetation, roads, and soil surfaces.

2.2 Internally Generated Data

In the simulation of realistic scenarios, the type, location, and orientation of the sensor, and the types and locations of vegetation, roads, bodies of water, etc, must be explicitly specified. The following files are generated or edited in the CREATION program or its modular FED:

- Feature maps are raster representations of the data required to define the scene content for vegetation, soil types, rocks, roads, and bodies of water in the DMA digital elevation area.
- Color spectral files are required for image synthesis. The inputs describe color and lighting model parameters, such as ambient, diffuse, and specular lighting properties, as well as the shininess of surfaces (high-lighting) for the principal background and target components, exclusive of the deciduous and coniferous trees. (The trees have their color and

lighting properties specified within their own modeling input data files.) The emissivities and reflectivities within the 3 to 5 and 8 to 12 μm bands are also defined in these files.

- Object-attribute files describe munitions, targets, and nonsolar light sources. These files specify target geometry, target thermal prediction, target camouflage pattern, and target position. The target position file specifies its position and orientation with respect to its three translational and three rotational degrees of freedom for given instants in time. The positions and orientations of munitions and up to seven independent, nonsolar light sources are similarly specified. The munitions effects are defined according to the combined obscuration model for battlefield-induced contaminants (COMBIC) [8] types. The red, green, and blue (RGB) color specifications of each munitions smoke and the independent light-source colors are defined in the object-attribute files, along with general lighting characteristics for movable point sources and spotlights.
- Target (visible) camouflage patterns may be either predefined camouflage or user-created patterns.
- Camera (sensor) position file data are similar to the position file data for the target. The sensor position, orientation, and field of view determine what will be seen at any instant.
- Atmospheric-transmission parameter file inputs control atmospheric-transmission effects through specification of properties such as humidity, rate of precipitation, reference altitude, and wavelength limits. These internal atmospheric model inputs can be either empirical or modeled with a variety of other atmospheric-transmission models (e.g., LOWTRAN or MODTRAN).
- Sensor-simulation data files consist of several preexisting sensor files, or the user may create new sensor-simulation data files by following the recommendations and specifications described in the CREATION user's manual.

3. CREATION Internal Models and Processes

3.1 Tree Geometry Model

For realistic high-resolution rendering of battlefield scenes with natural backgrounds, an accurate representation of vegetation geometry is needed, especially for trees. We prefer an algorithmic method of generating tree geometries using a compact parametric representation for simulating many separate species and instances of each species [9]. The tree geometry model should generate and efficiently render realistic foliage so that large numbers of individual trees can be included in the background scenes when needed. The model should be easy to use: the user should not need to rely on nonintuitive inputs or highly mathematical approaches requiring the solution of complex equations to specify and control the shapes of the trees. (Fractal approaches usually only apply when vegetation is self-similar, while botany-based models are very difficult to use for those who are not structural botanists.) Instead, the tree geometries should be based on the directly observable characteristics that distinguish various tree shapes from one another. The CREATION tree model meets these criteria by the adoption of a hierarchical rule-based methodology that divides branching levels into structural hierarchies from the main trunk down to the level of the smallest branches and leaves.

3.1.1 General Modeling Approach

The structure of a tree is visualized as a primary trunk, a variably curved structure similar to a cone. In some trees, this single structure may split multiple times along its length, forming additional similarly curved structures, which can likewise split along their length. This is how dichotomous branching is visualized. The attributes of these clones closely match those of the parent branch from the point of bifurcation except that clones are generated from different random seeds. After splitting, some clones will tend to curve more to compensate for the directional change caused by the splitting angle.

Monopodial (or "child") branches, which continue in line from a parent branch, are formed from the trunk and any existing clones. These branches can have entirely different attributes from their "parents." Many attributes, such as length, are defined relative to the corresponding attribute of the parents. For example, a child branch length is specified as a fraction of its parent length. These child branches can have subbranches and so on. For realistic, high-resolution simulation, these levels of recursion can be generally limited to three or four. Note that nearly all the other models that we researched consider each branching, whether monopodial or dichotomous, to be a discrete level. The other models often require nine or ten of these levels. While this branching is primarily a descriptive convention, the reduced number of recursion levels will be significant in optimized rendering (see sect. 3.1.5). Branch-level control can also assist the user in designing a particular tree.

The characteristic shape of specific trees is usually the result of the lengths of the primary branches according to their position on the trunk of the tree; e.g., a conically shaped tree has larger main branches near the base of the trunk. Alternatively, it is sometimes easier to define the general shape of the crown by envisioning an invisible envelope around the tree that inhibits branch growth. In addition, many trees have branches that almost always curve vertically (either up or down), presumably responding to the competing influences of light and gravity.

Cross-sectional variations can be particularly noticeable in the trunk. The scale of the cross section does not necessarily taper linearly as with a perfect cone. For example, some cacti have periodic variations of cross section in addition to simple random variations. The radial distance around any particular cross section can also vary randomly or periodically; i.e., the cross sections are not necessarily circular. In addition, the radius of the trunk clearly rapidly increases (flares) at the base of many trees.

Wind-induced tree movement is simulated in the CREATION tree model. The wind causes complex oscillatory motion throughout the tree that varies in amplitude and frequency, depending upon the wind velocity (wind force), elastic properties of the wood, and the length and thickness of the trunk and branches. These motions can be important considerations in dynamic imagery in which tree motions can distract human observers or confuse motion-cuing algorithms, which are used in some ATRs.

The principal structural and physical characteristics discussed in the previous paragraphs were incorporated into the CREATION tree model. Most of the significant geometric properties of a great variety of trees, shrubs, and bushes can be incorporated into any simulation that requires natural environments. Figure 2 shows various trees rendered with the model.

3.1.2 Tree Creation

The usual approach to creating trees within CREATION is to begin by deactivating the rendering of all levels but the first (the trunk). Once the trunk appearance is acceptable, the modeler then proceeds to activate and design the second level, and so on, in ascending degrees of complexity to the third and fourth levels. This approach allows the modeler to view the general shape and structure of the tree without the visual confusion and performance penalty caused from drawing minor branches and leaves. This selective control allows users to create and modify trees to optimize realism and rendering efficiency. In many cases, the modeler can draw foliated trees reasonably well in a final rendering without displaying any of the minor (third and fourth level) branches.

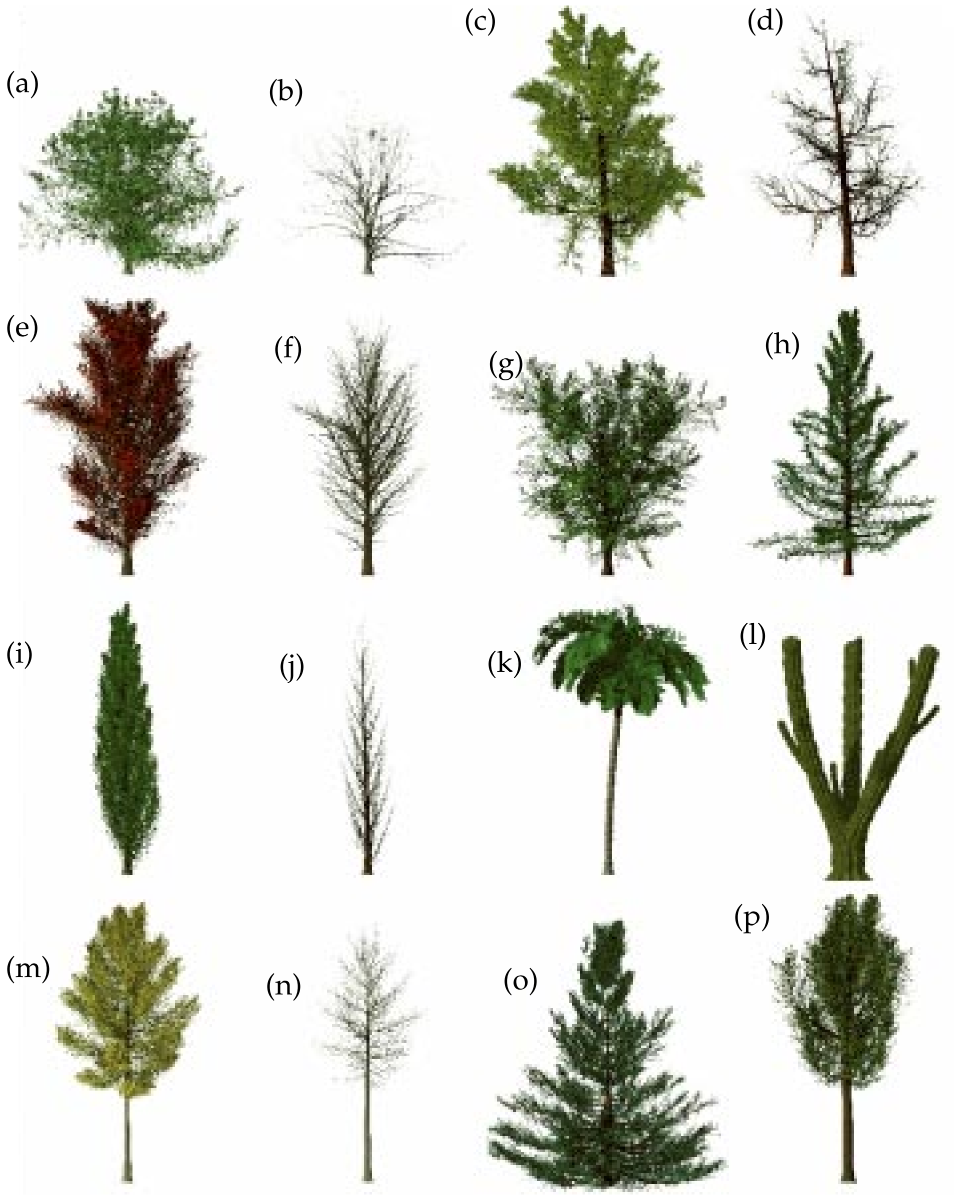

Figure 2. Examples of trees generated with CREATION tree model: (a) black oak, foliated and (b) black oak, bare; (c) black tupelo, foliated and (d) black tupelo, bare; (e) swamp oak, foliated and (f) swamp oak, bare; (g) cottonwood; (h) tamarack; (i) Lombardy poplar, foliated and (j) Lombardy poplar, bare; (k) queen palm; (l) generic cactus; (m) quaking aspen, foliated and (n) quaking aspen, bare; (o) balsam fir; and (p) white cedar.

The appendix lists most of the parameters we currently use in our CREATION tree model. Those readers who have access to a Silicon Graphics workstation and an Internet connection may wish to experiment interactively with the "VIEWTREE" demo program.* (Weber and Penn [9] explain more thoroughly the intuitive multicharacter variable names used in the parameter files shown in the appendix.) Many of the parameters are repeated for each level of recursion to permit greater control and flexibility. Additional parameters, mostly dealing with seasonal color and lighting properties, we have not listed or discussed. Where necessary, parameters are prefixed by a number that distinguishes similar parameters at different levels of recursion. Many parameters are followed by a variation parameter with the same name and a V suffix, such as 2Length and 2LengthV. The variations are usually positive numbers indicating the

**The VIEWTREE demo program is found on the ARL-Signature Modeling Branch Home Page: http://aaron.arl.mil. The demo requires a Silicon Graphics workstation (GL graphics/IRIX OS version 4.05 or higher).*

magnitude of the variation about the previous parameter. Since a few special trees, like palms, have exceptional geometric characteristics with respect to most other trees, some parameters use the negative sign as a flag to activate a special mode. All angular parameters are specified in degrees. Likewise, angles in the equations are in degrees, unless otherwise stated. Generally, the algorithms and equations describe structures based on extensive physical observations and research in tree reference manuals (see bibliography).

In addition, the appendix includes three tree parameter lists given for comparison. These specifications were designed based on observed geometric characteristics from a variety of illustrations and photographs in tree reference manuals and field observation of actual vegetation. Some of these trees, the California black oak and the quaking aspen, are shown, with and without leaves, in figures 2a, 2b, 2m, and 2n. A black tupelo tree with and without leaves is shown in more detail in figure 3. Because trees vary widely and can be hard to identify even by experts, these specific definitions can be used with little or no modification to represent many different species of similar-appearing trees. Figure 4 is a schematic diagram demonstrating some of the modeling parameters. The diagram does not show a complete tree, but rather exaggerates certain components to clarify their construction. Short descriptions of each input parameter are found in the appendix.

3.1.3 Leaves

Leaves assume many different shapes. A few common leaf geometries are available based on the LeafShape parameter. This parameter is an index to a list of predefined leaf shapes, such as oval, triangle, three-lobed oak, three-lobed maple, five-lobed maple, and three leaflets. These predefined leaf geometries are stored with unit width and length. Each shape can be sized and independently scaled for length and width to increase the number of leaf sizes and shapes. For optimum coverage versus computational expense, oval leaves are most commonly used.

Figure 3. Black tupelo, bare and with leaves.

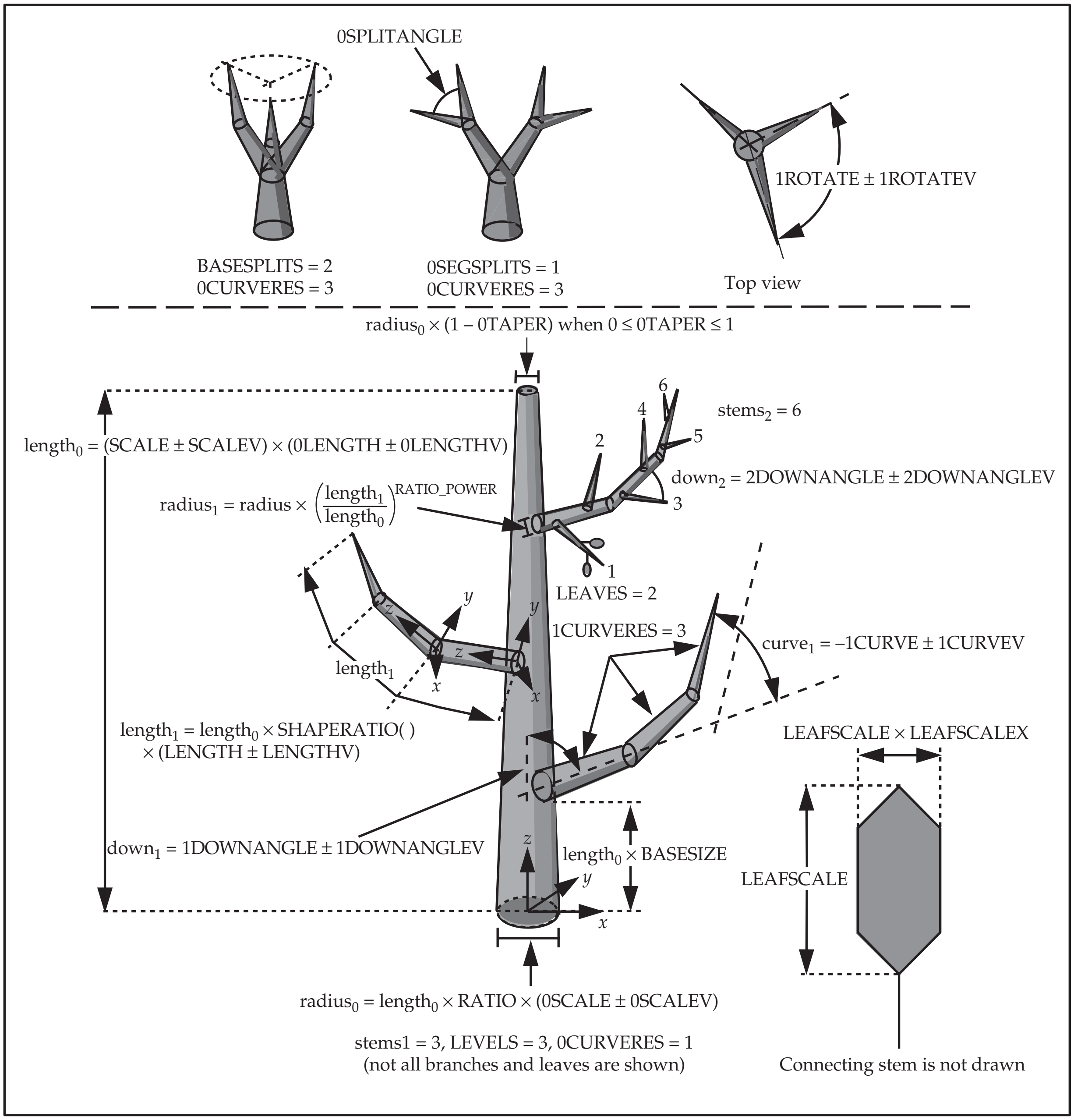

Figure 4. Schematic tree diagram.

3.1.4 Wind-Driven Tree Oscillation

Stem bending is modeled as the deflection of an elastic rod fixed on one end with a tapering circular cross section. This rod has a uniformly distributed force applied to it. Modeling this stem bending is a classical mechanics problem in which applying the Myosotis method for more complex shapes and tapering cross sections yields useful solutions for the deflection [10]. We then consider this rod a kind of elastic pendulum [11]. The entire system is then modeled as the superposition of coupled oscillators with different oscillatory periods and phase angles, so that the paths of points on a stem are very complex Lissajous figures [12]. These general results confirm our empirical observation that light to moderate winds induce trees to move so that branches sway in various directions and at different rates of oscillation. Higher velocity winds decrease the frequency of oscillation of the main branches until the frequency approaches zero, when the tree is strongly deflected in the direction of the wind force. We currently model the oscillatory effects observed for light to moderate winds only.

In our tree model, we simulate branch (and trunk) movement by introducing time-variant curvature changes to the stem segments. This effect is added to the structural curvature introduced by *n*Curve and *n*CurveBack resulting in rotations between segments about both the *x*- and *y*-axes. With wind speeds varying from wind speed to the sum of wind speed and wind gust, the sway angles, sway_x and sway_y, at unit position Z from 0 to 1 of a segment along the length of a stem are computed in seconds with the following equations, which use variables derived from variable names in the source code:

$$a_0 = [4 \times \text{length}_{\text{stem}}\,(1 - Z)]/\text{radius}_Z \quad \text{(degrees)}$$

$$a_1 = (\text{wind}_{\text{speed}}/50) \times a_0 \quad \text{(degrees)}$$

$$a_2 = [(\text{wind}_{\text{gust}}/50) \times a_0] + a_1/2 \quad \text{(degrees)}$$

$$b_x = \text{sway\_offset}_x + [(\text{radius}_{\text{stem}}/\text{length}_{\text{stem}})] \times \text{time}/15 \quad \text{(radians)}$$

$$b_y = \text{sway\_offset}_y + [(\text{radius}_{\text{stem}}/\text{length}_{\text{stem}})] \times \text{time}/15 \quad \text{(radians)}$$

$$\text{sway}_x = [a_1 \times \sin(b_x) + a_2 \times \sin(0.7 \times b_x)]/n\text{CurveRes} \quad \text{(degrees)}$$

$$\text{sway}_y = [a_1 \times \sin(b_y) + a_2 \times \sin(0.7 \times b_y)]/n\text{CurveRes} \quad \text{(degrees)}$$

The angles sway_offset_x and sway_offset_y are randomly selected for each stem in the tree. When the wind sway is activated, each tree geometry description must be reformed for each frame in an animation to adapt to the new angles. If the same random seed is used, a specific tree will always have the same basic geometry, perturbed only by the wind-activated curvature variations. The angles sway_x and sway_y cause rotations between segments about the *x*- and *y*-axes, respectively.

3.1.5 *Degradation at Range*

A tree generated with CREATION algorithms may have from 5,000 to 100,000 facets. The detail can be increased automatically for even higher resolution images. Currently, a high-end graphics workstation may be capable of only about 50,000 facets in real time. This potentially high tree-facet count is necessary for an accurate geometric representation at close ranges of 10 to 50 m or in equivalent magnified views at greater ranges, as in narrow fields of view. However, at longer ranges, such as 1000 m, a much lower resolution tree is rendered faster with little or no discernable change in shape.

Initially, forming multiple geometric descriptions of the same tree at different "levels of detail may seem useful." At longer ranges, progressively lower resolution geometric descriptions would be used. This simple approach has two problems. First, each instance of a tree requires computer system resources. The geometric description of an average tree typically requires approximately 1 MB of RAM. Also, 1 to 10 s may be required to generate the data. These numbers become much more significant when multiplied by, perhaps, 100 instances. While such numbers may be manageable on a fast graphics workstation with large amounts of memory, a more critical second problem arises with this fairly coarse quantization of the resolution. In a still picture, the changes between resolutions will not be very apparent, since the variably resolved trees appear as different trees. However, in a dynamic simulation, specific trees would, at some discrete range, suddenly switch from one resolution-determined geometry to the next. This will cause wide "resolution waves" to propagate through forest canopies as the viewer moves above the trees. These artifacts are unacceptable for realistic dynamic simulations.

A method is needed that uses a single geometric description, smoothly reinterprets this geometry according to range, and renders it at an optimal resolution for any range. The changes between the ranges of resolved geometries must be very fine, preferably corresponding to removal or modification of each facet, one at a time. There should be negligible computational overhead (CPU time and RAM) required with the change in rendering the specified geometry for the process to be worth undertaking instead of a brute-force rendering approach.

Since trees have highly structured, hierarchical geometries and are not arbitrary objects, a range-degradation algorithm can be designed to exploit their expected geometry. Each tree geometry is organized into four discrete hierarchical geometric descriptions: three stem levels and the leaves. Any stems beyond the third level are grouped with the third level. The higher level (smaller) stems are rarely visible at long ranges and are often obscured by the leaves. Oppenheimer recognized that polygonal tubes could be used for large-scale details and vectors (lines) for the smaller details [13]. He warns that artifacts can occur if the "cutover" level is not deep enough. He also states that many small branches can be rendered as triangular tubes. Our methods make similar approximations for rendering efficiency.

The technique used in CREATION does not convert the geometry—it simply reinterprets it to use the CPU and memory most efficiently. With progressively increasing ranges, a tree geometry will be reinterpreted so that polygonal stem meshes are replaced with lines and leaf polygons with points. With even longer ranges, some individual stems and leaves will disappear altogether. The specific geometry at any range can be properly rendered by the alteration of limits and increments in the loops that draw the data. Although individual stems and leaves disappear, they are not actually marked or deleted. Instead, the loop parameters that scan the stored geometry are changed so that items are skipped. Any number of arbitrarily ranged trees can be drawn in any order. The CPU time and memory overhead required to compute and store these boundary limits is negligible. This technique allows vast expanses of trees at longer ranges to be drawn very quickly. For example, a 100,000-facet tree geometry can be rendered at 2 km with about 30 lines and 1000 points. A viewer can then continuously move closer to any of these trees and see them become smoothly and naturally more detailed, until they are at their full resolution.

Since the items in each geometric description are ordered in the same manner as they were created, they generally start from the bottom of the tree and proceed upward. While these items are systematically organized, objects cannot be simply removed in order one at a time from the top or bottom of the list. This would, most probably, cause the top of the tree to be heavily degraded, while the bottom remained unchanged, or vice versa. Instead, the items of a type of geometry are organized into small groups called "masses." The number of elements per mass is defined in the source code by an appropriate constant called "mass_size." A mass_size of 16 for all the stems and 4 for the leaves is used. Curve-fitting equations yield a value between 0 and the mass_size. In the pseudo code that follows, the general term "primitive" refers to graphics elements (polygons, lines, or points) and the general term "item" refers to tree structures (leaves, trunk, branches, or subbranches). The total number of elements in the geometric description of any item is given as "$\text{total\_number}_{\text{item}}$." Depending on the range from the observer, the graphics primitive used to draw these items may be simpler or more complex. For example, a branch at a closer range would be drawn as a polygon, whereas at a longer range, it might be drawn as a line. The portion of the tree to be drawn is specified by the noninteger "$\text{number}_{\text{primitive,item}}$," which is between 0 and $\text{mass\_size}_{\text{primitive,item}}$. For example, a $\text{mass\_size}_{\text{lines,1}}$ of 16 divides main branch lines into masses of 16. A $\text{number}_{\text{lines,1}}$ of 5 means that for every 16 cross sections of recursion level 1, lines will be drawn connecting the first five. Fractional numbers will draw an additional item for a percentage of the masses. If there were 160 main-branch cross sections (10 masses) and $\text{number}_{\text{lines,1}}$ of 5.3, then the first 30 percent of the masses would show 6 of 16 lines, and the last 70 percent of the masses would show 5 of 16 lines. A loop to draw the reduced portion of the items using a specific primitive would be as follows:

$$\text{int\_number}_{\text{primitive,item}} = \text{integer}(\text{number}_{\text{primitive, item}})$$

$$\text{masses}_{\text{primitive,item}} = \text{total\_number}_{\text{item}}/\text{mass\_size}_{\text{primitive,item}}$$

$$\text{change}_{\text{primitive,item}} = \text{masses}_{\text{primitive, item}} \times (\text{number}_{\text{primitive, item}} - \text{int\_number}_{\text{primitive,item}})$$

for each mass = 0 to mass = $\text{masses}_{\text{primitive,item}}$

```
{
    start = mass × mass_size_primitive,item
    end = start + int_number_primitive,item
    if mass < change_primitive,item
        end = end + 1
    for each index = start to index = end
        draw_primitive,item(index)
}
```

To compute the necessary $\text{number}_{\text{primitive,item}}$, convert the range to a calibrated scale. This adjusts for the current image size and vertical field of view. A modified range value r_2 is computed as

$$r_2 = \text{range} \times (1000/\text{height}_{\text{image}}) \times \text{field\_of\_view}/60.$$

This computation compensates for the effect of a telephoto lens that magnifies a tree so that it appears to be much closer.

The following expressions outline how $\text{number}_{\text{primitive,item}}$ is computed for different levels at different ranges. First, the user-assigned general quality factor (usually between 0 and 1) is used to determine general scaling factors s and d:

$$s = \text{quality}/2 \quad \text{tree is evergreen, or deciduous in summer and fall,}$$
$$s = \text{quality} \quad \text{otherwise;}$$
$$d = 100 \quad \text{in spring,}$$
$$d = 200 \quad \text{otherwise.}$$

Then, the polygons, lines, and points needed for each display item are computed according to range r_2 as follows:

Level 0 Stems (trunk):

Range	Result
$r_2 < 100s$	do not draw trunk lines (produces artifacts that appear as a seam)
$100s < r_2$	draw all trunk lines
$r_2 < 300s$	$\text{number}_{\text{polygons,0}} = \text{mass\_size}_{\text{polygons,0}}$
$300s < r_2 < 800s$	$\text{number}_{\text{polygons,0}} = \text{mass\_size}_{\text{polygons,0}} \times [1.5 - r_2/600]$
$800s < r_2$	$\text{number}_{\text{polygons,0}} = 0$ (draw no trunk polygons)

Level 1 Stems (main branches):

Range	Result
$r_2 < 200s$	$\text{number}_{\text{polygons,1}} = \text{mass\_size}_{\text{polygons,1}} \times [1.5 - r_2/600]$ (bounded 0 to $\text{mass\_size}_{\text{polygons,1}}$)
	$\text{number}_{\text{lines,1}} = \text{mass\_size}_{\text{lines,1}}$
$200s < r_2 < 2000s$	$\text{number}_{\text{polygons,1}} = 0$ (draw no main branch polygons)
	$\text{number}_{\text{lines,1}} = \text{mass\_size}_{\text{lines,1}} \times [2.2 - 1.2\,(r_2/200s)^{0.3}]$
$2000s < r_2$	$\text{number}_{\text{polygons,1}} = \text{number}_{\text{lines,1}} = 0$ (draw no main branches)

Level 2 Stems (other branches):

Range	Result
$r_2 < 50s$	$\text{number}_{\text{polygons,2}} = \text{mass\_size}_{\text{polygons,2}}$
	$\text{number}_{\text{lines,2}} = \text{mass\_size}_{\text{lines,2}}$
$50s < r_2 < 100s$	$\text{number}_{\text{polygons,2}} = \text{mass\_size}_{\text{polygons,2}} \times [2 - r_2/50s]$
	$\text{number}_{\text{lines,2}} = \text{mass\_size}_{\text{lines,2}}$
$100s < r_2 < 500s$	$\text{number}_{\text{polygons,2}} = 0$ (draw no secondary branch polygons)
	$\text{number}_{\text{lines,2}} = \text{mass\_size}_{\text{lines,2}} \times [2 - (r_2/100s)^{0.5}]$
$500s < r_2$	$\text{number}_{\text{polygons,2}} = \text{number}_{\text{lines,2}} = 0$ (draw no secondary branches)

Leaves:

Range	Result
$r_2 < d/4$	$\text{number}_{\text{polygons,3}} = \text{mass\_size}_{\text{polygons,3}}$
	$\text{number}_{\text{points,3}} = \text{mass\_size}_{\text{points,3}}$
$d/4 < r_2 < d$	$\text{number}_{\text{polygons,3}} = \text{mass\_size}_{\text{polygons,3}} \times [4/3 - r_2/(3d/4)]$
	$\text{number}_{\text{points,3}} = \text{mass\_size}_{\text{points,3}}$
$d < r_2$	$\text{number}_{\text{polygons,3}} = 0$
	$\text{number}_{\text{points,3}} = \text{mass\_size}_{\text{points,3}} \times [1.5 - r_2/2d]$ (minimum of 1)

The effects of these expressions can be seen in figure 5 and in table 1, which summarize the total number of triangles, lines, and points drawn at each range. Triangles refer to the triangular mesh elements that make up the polygons.

Figure 6 shows high-resolution simulated visual imagery of a generic landscape from two different points of view. We applied a moderate atmospheric haze to the image in Figure 6b.

Figure 5. Quaking aspen rendered at ranges 30 to 1200 m (listed in table 1), increasing from left to right with size scaled for comparison.

Table 1. Number of elements drawn at specific ranges on fully foliated quaking aspen.

	Number of elements drawn according to range from tree (m)						
Item drawn	5	30	60	120	240	600	1200
Level 0 triangles	1,440	1,440	1,440	1,440	1,440	760	0
Level 0 lines	0	0	0	36	36	36	36
Level 1 triangles	960	960	960	0	0	0	0
Level 1 lines	240	240	240	223	153	35	0
Level 2 triangles	17,736	14,580	0	0	0	0	0
Level 2 lines	5,912	5,912	5,363	2,648	0	0	0
Leaf triangles	53,248	53,248	49,800	28,200	0	0	0
Leaf points	13,312	13,312	13,312	13,312	11,944	1664	1664

(a) (b)

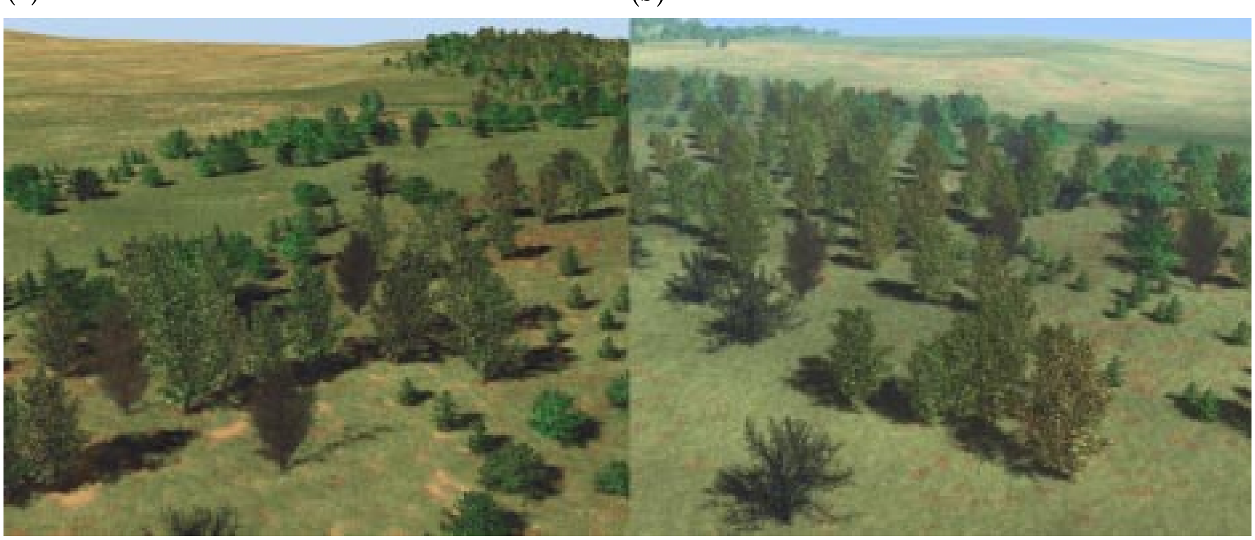

Figure 6. High-resolution scene from (a) northeast and (b) northwest.

3.2 Feature Editor

The CREATION scene generator requires explicit information about scene content to accurately render simulated imagery of actual test-site locations. The accurate rendering of actual high-resolution scenes requires a level of spatial resolution and specificity that is lacking in DMA digital feature analysis data (DFAD) [14]. For instance, DMA feature data consist of relatively large polygonal regions that permit five possibilities for vegetation coverage: bare, grassy, deciduous, coniferous, and mixed (deciduous and coniferous). While DFAD is a very efficient way to characterize terrain and store feature data, clearly for high-resolution simulations of ground-based or low-altitude flight imagery, it is not specific enough, since several kinds of grasses and various species of trees may be present in the field of view. The CREATION-produced synthetic imagery allows for 1 of 3 kinds of grass and up to 14 kinds of trees simultaneously available per sample cell to accommodate the scene complexity found in real-world imagery.

To produce specifically defined, high-spatial-resolution feature-map data, we developed the FED for the CREATION scene generation process. This FED enables modelers to create and edit various raster maps that are used as input data by the rendering software. It is essentially a specialized multilayer drawing program with a user-friendly interface to aid the bitwise manipulation of feature data for each terrain sample cell.

The CREATION FED can simultaneously load one or more of the four feature maps (vegetation, roads, water, and soil) in any combination (with or without the digital terrain elevation map) depending upon file sizes and the amount of RAM available. Each map can be individually edited as overlapping transparencies in which opacity can be user controlled in 256 increments (0 to 255) from perfectly transparent (0) to totally opaque (255). Currently, the terrain elevation data map is the only mapped data that the FED cannot modify. All other maps can be actively edited one at a time. Each feature map defines the placement of different background scene components with different data formats and bit pattern representations (colors). Each map has its own data-specific menu for setting the corresponding bit patterns. To edit a particular type of feature map, one must therefore toggle between different maps with their respective menus and color mappings by placing them on top of the stack of transparencies. This permits the skilled user to create or modify feature maps that are perfectly registered with respect to each other and the underlying elevation data.

A very useful aspect of the FED is its capability to use digitized top-down aerial photographs or satellite imagery as templates to create very accurate feature maps. These feature maps can be as accurate as permitted by the resolution of the aerial photographs or satellite imagery, the sample cell size (resolution) of the digital terrain elevation data, or the available RAM (during editing or execution of a scene file). Road maps, mineral and hydrological survey charts, and other area-specific data such as soil and vegetation types are also used when available. These additional data sources are very useful for eliminating ambiguities and enhancing information concealed in high overhead views with aerial photographic or satellite image data of, for example, grass and soil types under a dense tree canopy.

The capability to develop very accurate feature maps of actual locations is, of course, extremely important to the creation of high-resolution synthetic imagery of actual physical locations and is one of the strengths of the CREATION scene generation process. With this tool, the user can precisely tailor the scene content. The feature-mapped data along with specific scene file inputs (tree and grass types, area density, etc) control the location of every tree, bush, shrub, rock, road, and clump of grass within the background scene. The feature-mapped data with other input data control important aspects of ground-surface texturing.

3.3 Ground-Surface Texturing

The CREATION texture-mapping process produces controlled surface-conforming coarse, fine, and very fine textural effects. These effects include vegetation shadows, road surfaces, soil types, simplified water waves, and topographically specific hydraulic erosion (gullying). Vegetative ground-cover variations are applied according to the location and area density of the various types of grasses within the vegetation feature map. The color or temperature of the grass types is applied to the underlying ground as a texture. Individual grass blades are drawn when image resolution and fidelity require them. In those cases, the grass color or temperature is modulated by the properties of its underlying surface. For instance, grass drawn in areas shadowed by trees is modulated according to the darker shaded (color) or cooler (thermal) ground surface.

3.3.1 Overall Texturing Process

Texture mapping proceeds in four stages: (1) generating ground-surface texture differences, (2) producing hydraulic erosive effects (gullying), (3) drawing tree shadows projected to the surface according to solar inclination and azimuth angles, and (4) producing vegetative ground texturing to modulate assigned colors and temperatures to increase realism and to characterize the grass surface at ranges where resolution reduces the need to render individual grass blades.

The first texture mapping stage, generating ground-surface texture differences, is itself a multistage process depending on resolution that consists of three levels of detail: (1) generating gross surface texture over the entire mapped area (these patterns are generally at the scale of tens to hundreds of meters in diameter), (2) fine texture patterns applied with 16 times the resolution of the gross texture mapped pattern (about 1 to 10 m in diameter), and (3) very fine texture produced by generating a small texture pattern repeatedly applied to the same area as the second level, but with the addition of very fine-grained Gaussian random noise to diminish the otherwise objectionable pattern repetition (tiling) over larger areas. The magnitudes of all these effects are controllable through input values obtained from modeled or empirical data. The basic texture-generating algorithm is used for all three stages with the principal difference that finer textures are progressively superimposed and combined with larger scale effects according to spatial resolution and the magnitude of color or temperature differences. These ground-surface texture maps are smoothed by convolution at each stage, combined, and then convolved again.

The gully texture surface texture map is produced by drawing paths, starting at randomly selected source points, that follow the gradient of steepest descent. The drawing of tree shadows is accomplished by rendering a uniformly intense, reduced geometry tree as seen from the point of view of the light source, the sun in this case. The solar inclination and azimuth angles are determined according to the date, the time of day, and the longitude and latitude of the site. The shadows are projected to a planar shadow texture map. The vegetative surface texture map is produced by drawing areas of grass shaded according to grass type from the feature data and the color or temperature data for the respective grass type. The tree shadow, the gully, and the vegetative texture maps are each smoothed by convolution and combined with the ground-surface texture map and then convolved again.

Figure 7 shows the effect of the progressive addition of surface texture onto a bare uniform terrain followed by the sequential addition of grass and trees.

3.3.2 *Basic Texture Generating Algorithm*

The patterns generated in the first and second stages of the ground-surface texturing process are produced by a growth-rule-based algorithm that produces irregular, nonhomogeneous texture patterns. This algorithm emulates the growth and propagation of bacterial colonies or

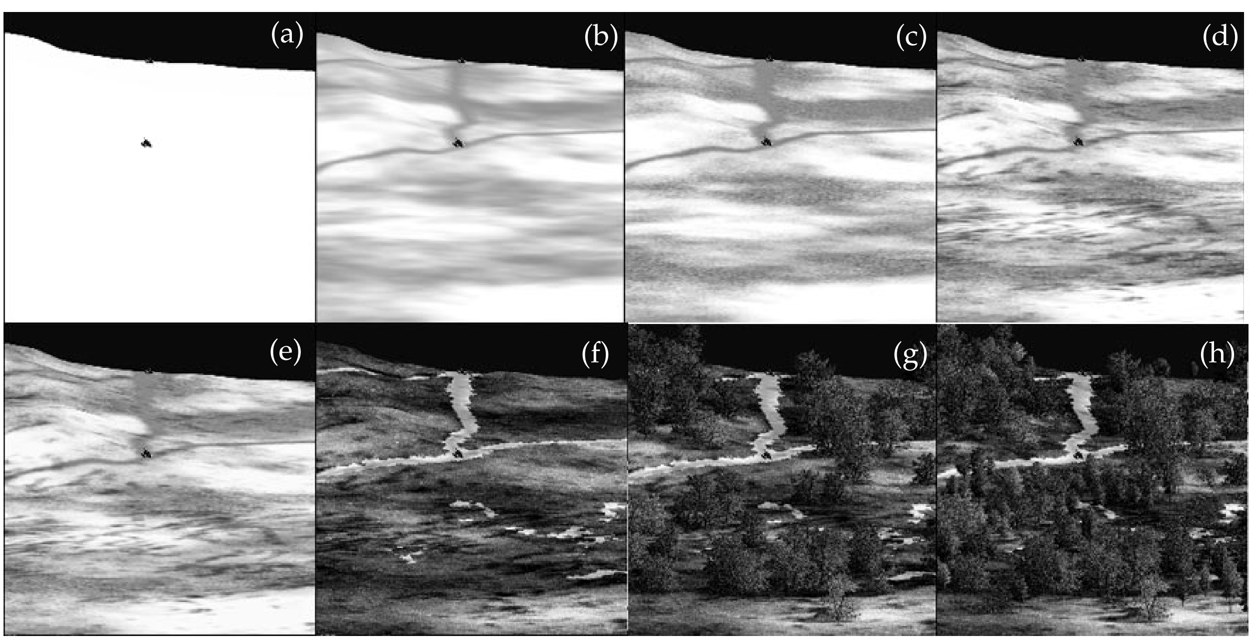

Figure 7. Progressive addition of surface textures (a–d) and grass and trees (e–h).

the diffusion of solutes in a solution. The algorithm is stochastic and begins with seed points randomly chosen over the entire area of the elevation data.

After a seed point is chosen, it spawns a small user-specified number of copies (MatTexture Splits) of itself at internally determined propagation angles from its clone(s) and propagation distances (MatTexture Displacement) from the parent. These lengths and angles are stochastically determined according to bounded Gaussian random values that the user chooses. Each of these spawned points can then generate further clones up to a user-determined number of growth iterations per colony or mass of points (MatTexture Depth). The process then repeats itself for another seed point at some other location. The total number of seed points is jointly controlled by the size of the area to be covered and the user input "MatTexture Density" factor. This process generates temperature or RGB shade modulated patterns that consist of random conglomerations of points, which tend to radiate outward from the seed point. The point patterns overlap and intersect one another dependent on the propagation angle, displacement length, etc. The entire ensemble of patterns is finally smoothed by convolution, yielding very natural-looking texture patches that are generally smooth and nonhomogeneous without sharp discontinuities. The texture pattern images in figure 8 were generated with the input values in table 2.

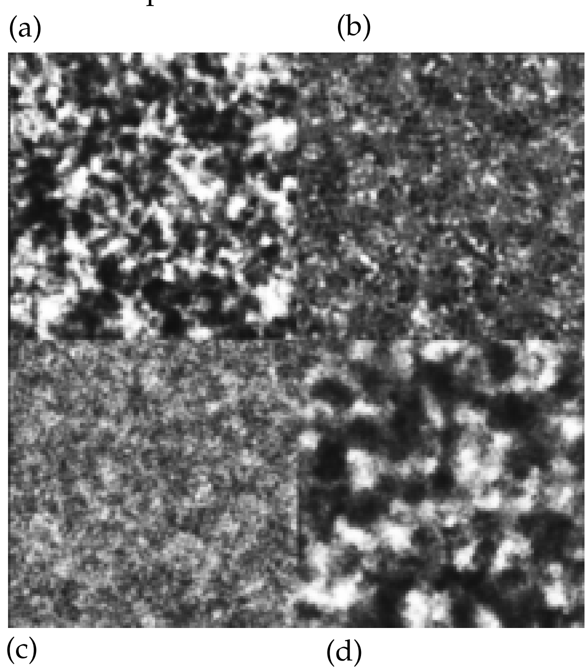

Figure 8. Texture patterns generated by CREATION with same random seed.

Table 2. Input values for texture patterns in figure 8.

MatTexture input variables	Texture patch input values in figure 8			
	a	b	c	d
Density	2	1	1	1
Splits	2	4	1	2
Depth	10	5	10	10
Displacement	10	10	10	10
Angle (°)	60	60	60	120

3.3.3 *Gully Texture*

The texture that emulates gullying is topographically specific; that is, the pattern is generated by finding the gradient of steepest descent from randomly assigned source points within the specific digital terrain elevation data. Hydraulic erosion occurs as water flows over a continuous surface from a source at a given point, following the “path of least resistance” or more specifically the path of steepest descent.

Let $z = f(x,y)$ be a function of two variables. The graph of $f(x,y)$ is a surface in R^3. The path of greatest rate of increase in height (steepest ascent) is found by

$$\nabla f\,(x,y) = \lim_{h \to 0} \frac{f\,(x+h,y) - f\,(x,y)}{h}\,\mathbf{i} + \lim_{h \to 0} \frac{f\,(x,y+h) - f\,(x,y)}{h}\,\mathbf{j} \qquad \text{(by definition).}$$

The gradient function generates a vector normal to the level contours that is oriented in the direction of greatest increase in slope. The negative value gives the opposite direction or the direction of steepest descent. In the discrete case, the elevations of the eight nearest neighboring positions are compared to a source point, the first test point and the lowest point found. A curved line is drawn through the source point to the lowest point. That point becomes the next test point, and its eight neighboring points are compared and its lowest neighbor found, repeating the process. When two or more equal-valued neighboring points are lower than the test point, then either point is randomly chosen. The process terminates for each gully path when no new neighboring points are found that are lower than the test point. A curved line is drawn through the points in sequence until the path is completed. This process repeats itself with a new source point until all of the paths are completed. Of course, actual erosion processes are much more complicated than this simplified model, since erosion depends on vegetative cover, soil properties, flow rates, and other geological and meteorological factors, in addition to the local gradient [15].

The gully algorithm ensures that the paths have a serpentine character resembling actual gullies. The erosion “depth” of the gully is controlled through its ΔT (temperature) or its normalized contrast value for color simulations. In a future implementation, gully troughs will actually modify the surface elevation.

3.4 Atmospheric Transmission and Battlefield Obscurants

The CREATION simulation package has a computationally efficient, simplified LOWTRAN-equivalent atmospheric-transmission model for the visible and infrared spectral bands that applies attenuation and scattering effects with input parameters that correspond to empirical meteorological data [16]. The atmospheric model also predicts altitude-dependent background sky radiance effects. Other atmospheric-transmission models can be used to postprocess atmospheric effects with the use of both the image and range-buffer output to calculate attenuation, scattering, etc.

The LOWTRAN-equivalent atmospheric-transmission model uses the range data to calculate attenuation according to the following equations:

Visible: $\tau = \exp(-\sigma R^B)$, $\sigma = \ln(\tau_{in})/R_{in}{}^B$, where τ is a transmission coefficient, σ is an attenuation coefficient, R is range, and B is a Beer's law coefficient.

Infrared: The infrared transmission coefficient table is calculated from the curve-fit algorithm LTR, LTR(hum, rain_rate, IR_trans_range, atm_pressure, altitude, λ_1, λ_2, weather_condition_index). The attenuation equation is then $T_{out}[y][x] = T_{air} + \tau(T_{in}[y][x] - T_{air})$, where T is temperature.

Figure 9 shows (a) a thermally modeled input image, followed by (b) the same image after a foggy atmosphere has been applied, and finally (c) the application of sensor effects to the image.

The CREATION simulation model also has a menu interface to define, locate, and set detonation or ignition times of various user-selected munitions or fires and their accompanying smoke clouds, and to define smoke cloud temperatures. The direction and speed of the wind parameters are used to process both visible and thermal obscurants by using the ARL Battlefield Environment Directorate (BED)/Grumman COMBICV battlefield obscurant model [8,17]. Figure 10, from dynamic simulations of an aerial attack on four ground vehicles, shows examples in the (a) visible and (b) the IR spectrum using applied battlefield obscurants, that is, smoke from oil fires (leading and trailing tank) and two phosphorus smoke obscurant clouds (two middle tanks). The field of view in the visible image is 20°, while the field of view in the infrared simulation is 10° (the gray scale distribution in these two images was nonlinearly modified to enhance contrast for printing). Also, note the difference in the visibility of the smoke plumes in the visible and the infrared simulated images.

3.5 Sensor, Optics, and Noise Modeling

CREATION scene generation software incorporates a powerful sensor simulation model that uses a superset of the FLIR92 sensor parameters and specifications to emulate the performance of a large variety of existing and prototypical thermal IR and visible sensor systems [18]. The model simulates optical blurring effects, including depth of field or focus, that vary according to aperture size, range to pixel, and position on the

(a) (b) (c)

Figure 9. (a) Input image with (b) atmospheric transmission and (c) sensor modeling applied.

Figure 10. Visible and IR simulations incorporating combat obscurants.

image plane, in addition to other optical aberration. Sensor-sampling effects are modeled when processing high-resolution images that have more than one pixel per instantaneous field of view (IFOV). Noise, particularly Gaussian shot noise, various detector nonuniformities and nonlinearities, and sensor scanning and sensor sampling artifacts found in actual systems are added in thermal sensor simulations. Our sensor simulation model can emulate the effects seen most often in first-generation forward-looking infrared (FLIR) systems, as well as those seen in more advanced systems. Alternatively, other sensor models can be used to postprocess stored output imagery (and range-buffer output) generated with the CREATION scene generator.

4. Applications of CREATION to Automatic Target Recognizer Testing

High-resolution simulated thermal imagery has many potential applications in the ATR community for scientific and engineering research and development, and testing of search algorithms. CREATION can, in addition to generating high-resolution optical (visible light and IR) imaging sensor output, generate advanced computer-aided design (ACAD) [19] facet files of backgrounds and embedded targets that can be used as geometric input to the Xpatch radar modeling software [20]. This unified multispectral modeling capability can be applied in testing ATRs in a wide variety of scenarios. These scenarios can range from simple single-frame simulations with one target in a background to highly complex dynamic simulations. These dynamic simulations can include aerial and ground attackers and defenders independently moving over a realistic battlefield, where obscurant clouds and naturalistic clutter from rocks, trees, bushes, and ground-surface textural variations can be realistically simulated.

The capability to precisely control the scenarios and the modular nature of CREATION allow modelers to systematically experiment with various prediction models under controlled conditions to test human search, recognition, and identification; missile seekers; and ground and low-altitude aerial combat ATRs, as well as to study the effects of partial concealment and various obscurants on recognition capabilities.

Other applications include image clutter-metrics research, in which the control of scene content is obviously beneficial. Another potential application is for mission planning and training, particularly for ground and low-altitude combat missions.

5. Conclusion

The CREATION simulation model is a set of programs that can efficiently produce large sequences of extremely high-quality output. In addition to its capability to synthesize accurately modeled thermal images, the CREATION scene generator program can simulate excellent high-resolution color imagery and generate facet files of natural backgrounds and embedded targets for radar modeling. This unified simulation capability has applications for training, mission planning, and scientific and engineering development of, for instance, ATR algorithms, human perception, and multispectral sensor modeling.

References

1. *Defense Mapping Agency Product Specifications for Digital Terrain Elevation Data (DTED)*. DMA Aerospace Center, 1986.
2. The Ballistic Research Laboratory CAD Package. Release 4.0. Ballistic Research Laboratory, Aberdeen Proving Ground, MD, 1991.
3. *Faceted Region EDitor (FRED) User's Manual*. U.S. Army Tank Automotive Research, Development, and Engineering Center (TARDEC) and Optimetrics, Inc., Warren, MI, February 1990.
4. *PRISM 3.1 User's Manual*. Keweenaw Research Paper. Keweenaw Research Center, Houghton, MI, 1993.
5. Johnson, Keith R. *Georgia Tech IR Signature Code (GTSIG) Analyst's Manual and User's Guide*. Georgia Technological Research Institute EML/EOD, Atlanta, GA.
6. Hummel, J., D. Longtin, N. Paul, and J. Jones. *Development of the Smart Weapons Operability Enhancement Interim Thermal Model: Technical Report*. Philips Laboratory, Geophysics Directorate, CO, 1991.
7. Balick, L., L. Link, R. Scoggins, and J. Solomon. *Thermal Modeling of Terrain Surface Elements: Technical Report*. Environmental Laboratory, U.S. Army Engineering Waterways Experiment Station (WES), Vicksburg, MS, 1981.
8. Hoock, Donald W., R. Sutherland, and D. Clayton. *Combined Obscuration Model for Battlefield-Induced Contaminants COMBIC.* ARL EOSAEL 87, Volume 11, October 1987.
9. Weber, J., and J. Penn. "Creation and Rendering of Realistic Trees." SIGGRAPH '95 *Computer Graphics Conference Proceedings, Annual Conference Series 1995.* ACM SIGGRAPH, Los Angeles, CA, August 1995, pp. 119–28.
10. den Hartog, J. *Strength of Materials*. Dover Publication, Inc., Mineola, NY, 1977, pp. 79–88.
11. Halliday, D., and R. Resnick. *Fundamentals of Physics*. 3d Edition. John Wiley and Sons, 1988, pp. 306–322.
12. Alonso, M., and E. Finn. *Physics.* Addison-Wesley, Reading, Massachusetts, 1970, pp. 160–166.
13. Oppenheimer, P. "Real Time Design and Animation of Fractal Plants and Trees." SIGGRAPH '86 *Computer Graphics Conference Proceedings, Annual Conference Series 1986.* ACM SIGGRAPH, Dallas, TX, 18–22 August 1986, pp. 55–64.
14. *Defense Mapping Agency Product Specifications for Digital Feature Analysis Data (DFAD) Level 1 and Level* 2. DMA Aerospace Center, 1986.
15. Watson, I., and A. D. Burnett. *Hydrology: An Environmental Approach*. Buchanan Books, Ft. Lauderdale, FL, 1993.

16. Kornfeld, G. H. "Theoretical and Experimental Justification for a Simplified LOWTRAN 6 Equivalent." *Proceedings of the Seventh EO-SAEL Meeting*. December 1986.

17. Gardner, Geoffrey Y. *Battlefield Obscurants Final Technical Report*. Grumman Data Systems Corp., Woodbury, NY, 10 September 1991.

18. Kornfeld, G. H. "Various FLIR Sensor Effects Applied to Synthetic Thermal Imagery." *Proceedings of the 1993 SPIE Conference*. April 1993.

19. *ACAD (Advanced Computer-Aided Design) User's Manual. Version 7.2*. Lockheed, Fort Worth Company, Fort Worth, TX, 1993.

20. *Xpatch User's Manual*. USAF Wright Laboratory/DEMACO, Inc., 1 June 1995.

Bibliography

Borisenko, A. I., and I. E. Tarapov. *Vector and Tensor Analysis With Applications.* Translated from the Russian by R. A. Silverman. Dover Publications, Inc., Mineola, NY, 1979, pp. 145–50.

Chan, F., F. Ching, W. Collins, M. Evans, et al. *Trees*. The American Horticultural Society, Mount Vernon, VA, 1982.

Collingwood, G., and W. Brush. *Knowing Your Trees*. 29th printing. The American Forestry Association, Washington, D.C., 1975.

De Reffye, P., C. Edelin, J. Françon, M. Jaeger, and C. Puech. "Plant Models Faithful to Botanical Structure and Development." *Computer Graphics Proceedings, Annual Conference Series, 1988*. ACM SIGGRAPH, Atlanta, GA, 1–5 August 1988. pp. 313–322.

Foley, J. D., A. van Dam, S. K. Feiner, and J. F. Hughes. *Computer Graphics: Principles and Practice.* 2d Edition, Addison-Wesley, Reading, MA, 1991.

Hora, B. *The Oxford Encyclopedia of Trees*. Crescent, 1986.

Johnson, K. *Thermal Contrast Model 2*. Georgia Technological Research Institute, 1990.

Peitgen, H.-O. and D. Saupe, Editors. *The Science of Fractal Images*. Springer-Verlag, New York, 1988.

Penn, J. A., H. Nguyen, T. Kipp, C. Kohler, G. Huynh, and M. Sola. "The CREATION Scene Modeling Package Applied to Theater Air Defense Fire Control Simulation, Multispectral Missile Seekers and Sensors." *Proceedings of the 1995 Conference on Multispectral Missile Seekers*. Huntsville, AL, November 1995.

Penn, J. A., H. Nguyen, M. Sola, C. Kohler, J. Weber, and S. Hawley. "The CREATION Scene Modeling Package Applied to Multispectral Missile Seekers and Sensors." *Proceedings of the 1995 National Fire Control Symposium*. Monterey, CA, 31 July–3 August 1995.

Prusinkiewicz, P., and A. Lindenmayer. *The Algorithmic Beauty of Plants.* Springer-Verlag, New York, 1990.

Symonds, G. *The Tree Identification Book*. William Morrow and Company, New York, 1958.

Weber, J., and J. A. Penn. *CREATION User's Manual, Version 1.27* (draft). U.S. Army Research Laboratory, Fort Belvoir, VA, November 1994.

Appendix. CREATION Tree Model Parameters Used to Generate Three Realistic Trees

The following parameter list includes modeling parameter inputs, along with brief descriptions of the function of each parameter, and the actual modeling parameter input values we used to create several of the trees illustrated in the main report. This list will prove especially useful for anyone with access to a Silicon Graphics workstation who chooses to experiment with the VIEWTREE demo on the Internet (http://aaron.arl.mil). These parameter names are the variable names used in the source code for the CREATION tree model. The schematic tree diagram, figure 4 in the main report, illustrates basic structural concepts and shows the spatial effects of the variables on tree structure. The quaking aspen, black tupelo, and the California black oak trees described by their modeling parameters are shown in figures 2 and 3 in the main report.

Parameter List

Parameter	Description	Quaking aspen	Black tupelo	California black oak
Shape	general tree shape index number	7	4	2
BaseSize	fractional branchless area at tree base	0.4	0.2	0.05
Scale, ScaleV, ZScale, ZScaleV	size and scaling of tree	13, 3, 1, 0	23, 5, 1, 0	10, 10, 1, 0
Levels	levels of recursion	3	4	3
Ratio, RatioPower	radius/length ratio, reduction	0.015, 1.2	0.015, 1.3	0.018, 1.3
Lobes, LobeDepth	sinusoidal cross-section variation	5, 0.07	3, 0.1	5, 0.1
Flare	exponential expansion at base of tree	0.6	1	1.2
0Scale, 0ScaleV	extra trunk scaling	1, 0	1, 0	1, 0
0Length, 0LengthV, 0Taper	fractional trunk, cross-section scaling	1, 0, 1	1, 0, 1.1	1, 0, 0.95
0BaseSplits	stem splits at base of trunk	0	0	2
0SegSplits, 0SplitAngle, 0SplitAngleV	stems splits, angle per segment	0, 0, 0	0, 0, 0	0.4, 10, 0
0CurveRes, 0Curve, 0CurveBack, 0CurveV	curvature resolution and angles	3, 0, 0, 20	10, 0, 0, 40	8, 0, 0, 90
1DownAngle, 1DownAngleV	main branch: angle from trunk	60, –50	60, –40	30, –30
1Rotate, 1RotateV, 1Branch	spiraling angle, number of branches	140, 0, 50	140, 0, 50	80, 0, 40
1Length, 1LengthV, 1Taper	relative length, cross-section scaling	0.3, 0, 1	0.3, 0.05, 1	0.8, 0.1, 1
1SegSplits, 1SplitAngle, 1SplitAngleV	stem splits per segment	0, 0, 0	0, 0, 0	0.2, 10, 10
1CurveRes, 1Curve, 1CurveBack, 1CurveV	curvature resolution and angles	5, –40, 0, 50	10, 0, 0, 90	10, 40, –70, 150
2DownAngle, 2DownAngleV	secondary branch: angle from parent	45, 10	30, 10	45, 10
2Rotate, 2RotateV, 2Branches	spiraling angle, number of branches	140, 0, 30	140, 0, 25	140, 0, 120
2Length, 2LengthV, 2Taper	relative length, cross-section scaling	0.6, 0, 1	0.6, 0.1, 1	0.2, 0.05, 1
2SegSplits, 2SplitAngle, 2SplitAngleV	stem splits per segment	0, 0, 0	0, 0, 0	0.1, 10, 10
2CurveRes, Curve, 2CurveBack, 2CurveV	curvature resolution and angles	3, –40, 0, 75	10, –10, 0, 150	3, 0, 0, –30
3DownAngle, 3DownAngleV	tertiary branch: angle from parent	45, 10	45, 10	45, 10
3Rotate, 3RotateV, 3Branches	spiraling angle, number of branches	77, 0, 10	140, 0, 12	140, 0, 0
3Length, 3LengthV, 3Taper	relative length, cross-section scaling	0, 0, 1	0.4, 0, 1	0.4, 0, 1
3SegSplits, 3SplitAngle, 3SplitAngleV	stem splits per segment	0, 0, 0	0, 0, 0	0, 0, 0

Parameter List (cont'd)

Parameter	Description	Quaking aspen	Black tupelo	California black oak
3CurveRes, 3Curve, 3CurveBack, 3CurveV	curvature resolution and angles	1, 0, 0, 0	1, 0, 0, 0	1, 0, 0, 0
Leaves, LeafShape	number of leaves per parent, shape index	25, 0	6, 0	25, 0
LeafScale, LeafScaleX	leaf length, relative x-scale	0.17, 1	0.3, 0.5	0.12, 0.66
AttractionUp	upward growth tendency	0.5	0.5	0.8
PruneRatio	fractional effect of pruning	0	0	0
PruneWidth, PruneWidthPeak	width, position of envelope peak	0.5, 0.5	0.5, 0.5	0.5, 0.5
PrunePowerLow, PrunePowerHigh	curvature of envelope	0.5, 0.5	0.5, 0.5	0.5, 0.5

Distribution

Admnstr
Defns Techl Info Ctr
Attn DTIC-OCP
8725 John J Kingman Rd Ste 0944
FT Belvoir VA 22060-6218

Ofc of the Dir Rsrch and Engrg
Attn R Menz
Pentagon Rm 3E1089
Washington DC 20301-3080

Ofc of the Secy of Defns
Attn ODDRE (R&AT) G Singley
Attn ODDRE (R&AT) S Gontarek
The Pentagon
Washington DC 20301-3080

OSD
Attn OUSD(A&T)/ODDDR&E(R) R Tru
Washington DC 20301-7100

CECOM
Attn PM GPS COL S Young
FT Monmouth NJ 07703

CECOM RDEC Elect System Div Dir
Attn J Niemela
FT Monmouth NJ 07703

CECOM
Sp & Terrestrial Commctn Div
Attn AMSEL-RD-ST-MC-M H Soicher
FT Monmouth NJ 07703-5203

Dept of the Army (OASA) RDA
Attn SARD-PT R Saunders
103 Army
Washington DC 20301-0103

Hdqtrs Dept of the Army
Attn DAMO-FDT D Schmidt
400 Army Pentagon Rm 3C514
Washington DC 20301-0460

MICOM RDEC
Attn AMSMI-RD W C McCorkle
Redstone Arsenal AL 35898-5240

Mission Rsrch, Dev, & Engrg Ctr
Attn AMSMI-RD-MG-IP S Motz
Redstone Arsenal AL 35898

US Army CECOM Rsrch, Dev, & Engrg Ctr
Attn R F Giordano
FT Monmouth NJ 07703-5201

US Army Edgewood Rsrch, Dev, & Engrg Ctr
Attn SCBRD-TD J Vervier
Aberdeen Proving Ground MD 21010-5423

US Army Info Sys Engrg Cmnd
Attn ASQB-OTD F Jenia
FT Huachuca AZ 85613-5300

US Army Materiel Sys Analysis Agency
Attn AMXSY-D J McCarthy
Aberdeen Proving Ground MD 21005-5071

US Army Matl Cmnd
Dpty CG for RDE Hdqtrs
Attn AMCRD BG Beauchamp
5001 Eisenhower Ave
Alexandria VA 22333-0001

US Army Matl Cmnd
Prin Dpty for Acquisition Hdqrts
Attn AMCDCG-A D Adams
5001 Eisenhower Ave
Alexandria VA 22333-0001

US Army Matl Cmnd
Prin Dpty for Techlgy Hdqrts
Attn AMCDCG-T M Fisette
5001 Eisenhower Ave
Alexandria VA 22333-0001

US Army Mis Cmnd
Attn AMSMI-RD-SS-HW J Cole
Redstone Arsenal AL 35898

US Army Missile Lab
Attn AMSMI-RD-SS-HW S Mobley
Redstone Arsenal AL 35809

US Army Natick Rsrch, Dev, & Engrg Ctr
Acting Techl Dir
Attn SSCNC-T P Brandler
Natick MA 01760-5002

US Army Rsrch Ofc
Attn G Iafrate
4300 S Miami Blvd
Research Triangle Park NC 27709

Distribution (cont'd)

US Army Simulation, Train, & Instrmntn Cmnd
Attn J Stahl
12350 Research Parkway
Orlando FL 32826-3726

US Army TACOM
Attn AMSTA-TR-S T Gonda
Mail Stop 263
Warren MI 48397-5000

US Army Tank-Automtv & Armaments Cmnd
Attn AMSTA-AR-TD C Spinelli
Bldg 1
Picatinny Arsenal NJ 07806-5000

US Army Tank Automtv Rsrch, Dev, & Engrg Ctr
Attn AMSTA-TA J Chapin
Warren MI 48397-5000

US Army Test & Eval Cmnd
Attn R G Pollard III
Aberdeen Proving Ground MD 21005-5055

US Army Train & Doctrine Cmnd
Battle Lab Integration & Techl Dirctrt
Attn ATCD-B J A Klevecz
FT Monroe VA 23651-5850

US Military Academy
Dept of Mathematical Sci
Attn MAJ D Engen
West Point NY 10996

USAASA
Attn MOAS-AI W Parron
9325 Gunston Rd Ste N319
FT Belvoir VA 22060-5582

Dept of the Navy
NAWCAD Atlantic Ranges & Facilities
Attn D Jackson
48150 Shaw Rd Unit 5
Patuxent River MD 20670-1907

Nav Air Warfare Ctr Weapons Div
Attn Code 45200E (P273) L Yu
Point Mugu CA 93042-5001

Nav Air Warfare Ctr Weapons Div
Attn Code SerC2951 (472210D)/9140 H Yang
China Lake CA 93555-6001

Nav Surface Warfare Ctr
Attn Code B07 J Pennella
17320 Dahlgren Rd Bldg 1470 Rm 1101
Dahlgren VA 22448-5100

GPS Joint Prog Ofc Dir
Attn COL J Clay
2435 Vela Way Ste 1613
Los Angeles AFB CA 90245-5500

DARPA
Attn B Kaspar
Attn L Stotts
3701 N Fairfax Dr
Arlington VA 22203-1714

ARL Electromag Group
Attn Campus Mail Code F0250 A Tucker
University of Texas
Austin TX 78712

Dir for MANPRINT
Ofc of the Deputy Chief of Staff for Prsnnl
Attn J Hiller
The Pentagon Rm 2C733
Washington DC 20301-0300

Palisades Instit for Rsrch Svc Inc
Attn E Carr
1745 Jefferson Davis Hwy Ste 500
Arlington VA 22202-3402

Waterways Experiment Station
Attn J Ballard EN-C
3909 Halls Ferry Rd
Vicksburg MS 39180

US Army Rsrch Lab
Attn BED IS&TD R Shirkey
White Sands Missile Range NM 88002

US Army Rsrch Lab Elec Warfare Div
Attn AMSRL-SL-EM R Lebsock
White Sands Missile Range NM 88002

Distribution (cont'd)

US Army Rsrch Lab
Attn AMSRL-CI-LL Techl Lib (3 copies)
Attn AMSRL-CS-AL-TA Mail & Records Mgmt
Attn AMSRL-CS-AL-TP Techl Pub (3 copies)
Attn AMSRL-IS J D Gantt
Attn AMSRL-IS P Emmerman
Attn AMSRL-IS-CI P David

US Army Rsrch Lab (cont'd)
Attn AMSRL-SE J M Miller
Attn AMSRL-SE J Pellegrino
Attn AMSRL-SE-SE C Kohler
Attn AMSRL-SE-SE J Colby
Attn AMSRL-SE-SE J Penn
Attn AMSRL-SE-SE T Kipp
Adelphi MD 20783-1197

REPORT DOCUMENTATION PAGE

Form Approved OMB No. 0704-0188

Public reporting burden for this collection of information is estimated to average 1 hour per response, including the time for reviewing instructions, searching existing data sources, gathering and maintaining the data needed, and completing and reviewing the collection of information. Send comments regarding this burden estimate or any other aspect of this collection of information, including suggestions for reducing this burden, to Washington Headquarters Services, Directorate for Information Operations and Reports, 1215 Jefferson Davis Highway, Suite 1204, Arlington, VA 22202-4302, and to the Office of Management and Budget, Paperwork Reduction Project (0704-0188), Washington, DC 20503.

1. AGENCY USE ONLY *(Leave blank)*	2. REPORT DATE	3. REPORT TYPE AND DATES COVERED
	April 1998	Interim, from July 1996 to July 1997

4. TITLE AND SUBTITLE
CREATION Scene Generation for ATR Applications

5. FUNDING NUMBERS
DA PR: A305
PE: 61102A

6. AUTHOR(S)
Hung M. Nguyen, Joseph A. Penn, Teresa A. Kipp, Giap D. Huynh, and Janice F. Colby

7. PERFORMING ORGANIZATION NAME(S) AND ADDRESS(ES)
U.S. Army Research Laboratory
Attn: AMSRL-SE-SE (email: mhung@arl.mil)
2800 Powder Mill Road
Adelphi, MD 20783-1197

8. PERFORMING ORGANIZATION REPORT NUMBER
ARL-TR-1489

9. SPONSORING/MONITORING AGENCY NAME(S) AND ADDRESS(ES)
U.S. Army Research Laboratory
2800 Powder Mill Road
Adelphi, MD 20783-1197

10. SPONSORING/MONITORING AGENCY REPORT NUMBER

11. SUPPLEMENTARY NOTES
AMS code: 611102.305
ARL PR: 7NE0N1

12a. DISTRIBUTION/AVAILABILITY STATEMENT
Approved for public release; distribution unlimited.

12b. DISTRIBUTION CODE

13. ABSTRACT *(Maximum 200 words)*

The CREATION (computer generation of realistic environments with atmospheres for thermal imagery with optics and noise) scene simulation program produces high-quality three-dimensional imagery of realistic battlefield environments.

Several important methodologies used in the CREATION program are discussed. These include efficient ground-texturing techniques that use growth-rule-based texture patterns and gradient-of-steepest-descent algorithmic erosion processes to increase the realism of low-resolution Defense Mapping Agency (DMA) digital terrain elevation data (DTED). Methods discussed include algorithms to produce very realistic three-dimensional trees that are succinctly described by a small number of geometrical parameters and efficiently rendered. Discussion of the vegetation model also includes a description of algorithms to efficiently render large masses of trees that smoothly and seamlessly increase in detail as the viewer continuously approaches them.

14. SUBJECT TERMS
Thermal scene background, tree geometry model, visible scene backgrounds

15. NUMBER OF PAGES
39

16. PRICE CODE

17. SECURITY CLASSIFICATION OF REPORT	18. SECURITY CLASSIFICATION OF THIS PAGE	19. SECURITY CLASSIFICATION OF ABSTRACT	20. LIMITATION OF ABSTRACT
Unclassified	Unclassified	Unclassified	UL

NSN 7540-01-280-5500

Standard Form 298 (Rev. 2-89)
Prescribed by ANSI Std. Z39-18
298-102